

Analytical Dirac-Hartree-Fock-Slater screening function for atoms ($Z = 1-92$)

F. Salvat, J. D. Martínez, R. Mayol, and J. Parellada

Departament d'Estructura i Constituents de la Matèria, Facultat de Física, Universitat de Barcelona, Diagonal 645, 08028 Barcelona, Spain

(Received 12 December 1986)

An analytical approximation, depending on five parameters, for the atomic screening function is proposed. The corresponding electrostatic potential takes a simple analytical form (superposition of three Yukawa potentials) well suited to most practical applications. Parameters in the screening function, determined by an analytical fitting procedure to Dirac-Hartree-Fock-Slater (DHFS) self-consistent data, are given for $Z = 1-92$. The reliability of this analytical approach is demonstrated by showing that (a) Born cross sections for elastic scattering of fast charged particles by the present analytical field and by the DHFS field practically coincide and (b) one-electron binding energies computed from the independent-particle model with our analytical field (corrected for exchange and electrostatic self-interaction) agree closely with the DHFS energy eigenvalues.

I. INTRODUCTION

Quite a number of problems related to atomic structure and radiation transport can be quantitatively solved in terms of the atomic screening function $\phi(r)$. This function is defined as the ratio between the electrostatic potential $U(r)$, experienced by an infinitesimal point charge at a distance r from the nucleus (spherical symmetry is assumed), and the electrostatic potential of the bare nucleus. Considering the nucleus as a point charge, $U(r)$ can be calculated in terms of the atomic electron density $\rho(r)$ as

$$U(r) = -\frac{Z}{r} + \int_{r>} \frac{\rho(r')}{r'} d^3r' \equiv -\frac{Z}{r} \phi(r), \tag{1}$$

where Z is the nuclear charge and $r_{>}$ is the greater of r and r' (the atomic unit system, $\hbar = m = e = 1$, is used throughout this paper). Poisson's equation links $\rho(r)$ and $\phi(r)$ through

$$\rho(r) = \frac{Z}{4\pi r} \phi''(r). \tag{2}$$

Different approximate analytical screening functions for neutral atoms have been proposed in the literature.¹⁻⁷ Almost all of these proposals rely on the Thomas-Fermi (TF) statistical model of the atom; only a few exceptions are based on self-consistent Hartree-Fock (HF) or Hartree-Fock-Slater (HFS) calculations.

An important application of these screening functions is in independent-particle model (IPM) calculations of atomic structure. The IPM one-electron orbitals and binding energies are obtained by solving the Schrödinger equation for a central potential $V(r)$, giving the average interaction energy of an atomic electron at a distance r from the nucleus with the nuclear charge and with the other $Z - 1$ electrons. The potential

$$V(r) = U(r) - V_{\text{ex}}(r) \tag{3}$$

differs from (1) in the term $V_{\text{ex}}(r)$, usually referred to as the exchange potential, which accounts for exchange

effects and removes from $U(r)$ the electrostatic self-interaction of each electron. The exchange correction is usually introduced by using Slater's⁸ approximation, i.e., from the free-electron-gas theory, which affords a local expression for it in terms of the electron density $\rho(r)$:

$$V_{\text{ex}}(r) = \frac{3}{2} \alpha_X \left(\frac{3}{\pi} \rho(r) \right)^{1/3}. \tag{4}$$

The value of the parameter α_X depends on the procedure used to derive $V_{\text{ex}}(r)$ from the HF theory. If the free-electron approximation is introduced in the expression of the exchange energy before variation, one finds $\alpha_X = 1$ which also coincides with the value obtained in the derivation of the Thomas-Fermi-Dirac equation (see, e.g., Ref. 8). Slater introduced the free-electron approximation in the HF exchange potential (i.e., after variation) and found $\alpha_X = \frac{3}{2}$. As a consequence, with $\alpha_X = \frac{3}{2}$, the eigenvalues of the radial equation have the significance of one-electron binding energies as in the HF theory (Koopmans' theorem). We shall adopt Slater's procedure which is usually satisfactory for ground configurations. It should be pointed out that Slater's potential (4) is not adequate at large distances from the nucleus; in that region, the electron density is very small, and (4) cannot compensate for the electrostatic self-interaction included in the electrostatic potential $U(r)$. In order to ensure the correct asymptotic behavior of $V(r)$,

$$rV(r) \xrightarrow{r \rightarrow \infty} -1, \tag{5}$$

Latter² adopted the following *ad hoc* prescription:

$$V(r) = -\frac{Z}{r} \phi(r) - V_{\text{ex}}(r), \text{ if } V(r) < -1/r$$

$$= -\frac{1}{r}, \text{ otherwise,} \tag{6}$$

to compute IPM one-electron binding energies for neutral atoms from the TF screening function. Latter's prescription (6) is usually adopted in HFS self-consistent calculations.

The HFS approximation, in which exchange effects are also introduced following Slater's approximation, plays a role midway between HF and TF models. HFS one-electron orbitals and binding energies are obtained by solving the Schrödinger equation for the self-consistent HFS potential, defined as in (6) with $\phi(r)$ computed according to (1) from the HFS electron density. The HFS potential is common to all the electrons. This is not so for the HF approximation where the one-electron orbitals are obtained (for closed-shell atoms) as solutions of Schrödinger equations with *different* effective potentials. Numerical HFS calculations have been carried out by Herman and Skillman⁹ for neutral atoms with $Z = 1-103$. Their results have been adopted to determine the parameters of an analytical IPM potential by Green, Sellin, and Zachor.⁶

Dirac-Hartree-Fock-Slater (DHFS) calculations,¹⁰ in which the one-electron orbitals are solutions of the Dirac equation instead of the Schrödinger equation, incorporate the main relativistic effects on the one-electron orbitals and binding energies in a natural way. To the best of our knowledge, no analytical screening functions incorporating relativistic effects have been proposed up to date, although distortions in the electron charge density and in the self-consistent potential due to these effects are noticeable even for intermediate atomic numbers.

In this work we propose a simple analytical approximation, $\phi_a(r)$ for the atomic screening function depending on five parameters which are determined analytically from the results of DHFS calculations. These screening functions, when used with the Slater exchange potential and Latter's correction (6), provide a simple and rather accurate analytical potential for IPM calculations on atomic structure. The universal TF screening function, mainly in the approximate analytical form suggested by Molière¹ which allows us to perform most calculations analytically, has been extensively used to treat a number of problems related with interactions of charged particles with atoms, including multiple scattering¹¹⁻¹³ and bremsstrahlung emission.¹⁴ Our screening functions, having the same functional form as Molière's, are particularly suitable for treating these problems by improving the Molière-TF approach without any additional complexity of the calculations. The present analytical approximation can be of great value to improve the description of elastic scattering events in Monte Carlo simulation of electron transport.¹⁵

The analytical screening function $\phi_a(r)$ is described in Sec. II. Parameters for $Z=1-92$ obtained from the DHFS self-consistent results following an analytical procedure described in the Appendix are given. Atomic form factors and Born scattering amplitudes for structureless charged particles derived from $\phi_a(r)$ are compared with numerical results from the DHFS density and from the other analytical approximations in Sec. III. Finally, Sec. IV is dedicated to the analysis of the reliability of IPM results based on these screening functions, including comparisons with other analytical IPM potentials.

II. ANALYTICAL SCREENING FUNCTIONS

Screening functions adopted in the literature are usually based on the TF model and its refinements. The most elemental TF model provides a universal screening function satisfying the following differential equation (see, e.g., Ref. 16):

$$\phi''_{\text{TF}}(x) = \frac{[\phi_{\text{TF}}(x)]^{3/2}}{x^{1/2}}, \quad (7)$$

where $x = r/b$ with $b = 0.88534Z^{-1/3}$. Accurate fits to ϕ_{TF}^{-1} using polynomials in $x^{1/2}$ have been proposed by Latter² and by Gross and Dreizler.³ Due to the failures of the statistical model in the regions of large potential gradients and of small electron densities, the TF screening function becomes unreliable at small and large distances from the nucleus.

Molière¹ used the following analytical approximation:

$$\phi_{\text{TF}}(r) = \sum_{i=1}^3 B_i \exp(-\beta_i r/b), \quad (8)$$

where

$$B_1 = 0.1, \quad B_2 = 0.55, \quad B_3 = 0.35,$$

$$\beta_1 = 6.0, \quad \beta_2 = 1.2, \quad \beta_3 = 0.3.$$

Function (8) differs from the exact solution of (7) by less than 0.002 in the range $0 < x < 6$. A similar analytical approximation has been proposed by Csavinszki⁴ on the basis of a variational solution of Eq. (7). The approximation (8) forces the exponential decrease of $\phi(r)$ for large r values which results from quantum treatments. This feature makes expression (8) more reliable for practical calculations than the exact TF screening function.

The analytical form (8) has also been adopted by Bonham and Strand⁵ to approximate the screening function for Thomas-Fermi-Dirac atoms; in this case the parameters B_i and β_i are continuous functions of Z which have been approximated by polynomials in $\ln Z$ by those authors. Simple analytical screening functions have also been given by Gross and Dreizler³ on the basis of the variational formulation of the Thomas-Fermi-Dirac-Weizsacker theory. Although the screening functions of Bonham and Strand and of Gross and Dreizler are undoubtedly more reliable than the TF one, the scaling properties of the simple TF theory are lost when exchange and gradient corrections are introduced. Once we renounce to these scaling properties, self-consistent methods that are more accurate than the statistical ones can be adopted to derive analytical screening functions.

Green, Sellin, and Zachor⁶ have introduced an IPM potential with the following analytical form:

$$V(r) = -\frac{1}{r} [(Z-1)\Omega(r) + 1], \quad (9)$$

where $\Omega(r)$ is a two-parameter screening function

$$\Omega(r) = [H(e^{r/d} - 1) + 1]^{-1}. \quad (10)$$

The parameters H and d have been obtained by Green, Sellin, and Zachor⁶ from a least-squares fitting of the po-

tential (9) to the HFS potential of Herman and Skillman.⁹ Alternative sets of parameters, determined by fitting the IPM eigenvalues obtained with the potential (9) to the HF eigenvalues and to experimental ionization energies, are also given in Ref. 6 for $Z=1-103$. More recently, the parameters of (9) have also been determined from a variational procedure in which the total binding energy of the atom, computed from a Slater determinant composed of one-electron orbitals, is minimized.⁷ It should be noted that $\Omega(r)$ in (9) stands for the electrostatic screening function, the differences between (9) and our potential (6) arising from the different approaches used to introduce the self-energy (and exchange) corrections.

The DHFS self-consistent calculations provide us with reliable screening functions accounting for relativistic effects which are difficult to be included in statistical or nonrelativistic self-consistent models. DHFS densities for neutral atoms, up to $Z=92$, have been computed using our own computer code.¹⁷ Spherical symmetry is assumed, so an average over open-shell orbitals is performed to obtain the electron density $\rho(r)$. Central field orbitals are obtained by solving the Dirac radial equations for the HFS potential with Latter's correction [Eqs. (3)–(6) with $\alpha_X = \frac{3}{2}$].

Representation of the DHFS screening functions in a semilogarithmic plot (Fig. 1) reveals a nearly linear behavior for large radial distances which suggests that they can be adequately fitted with the analytical form adopted by

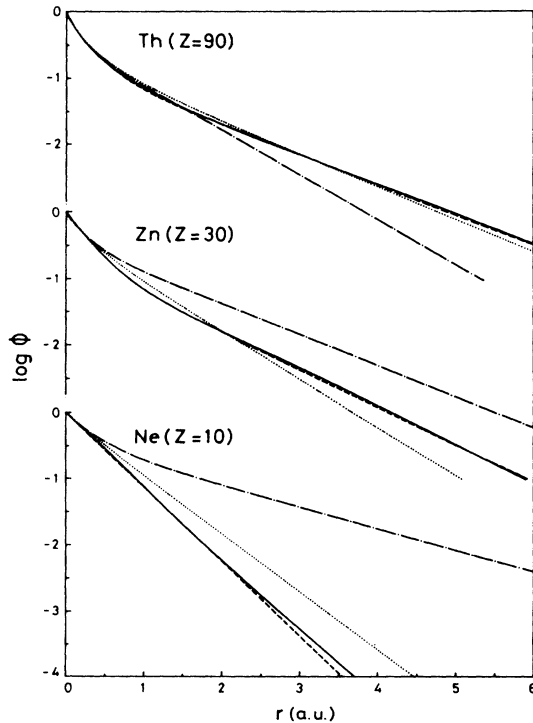


FIG. 1. Screening functions for Ne, Zn, and Th ($Z=10, 50$, and 90). The solid curves are the DHFS results. The dashed, dotted, and dash-dotted curves correspond to the analytical screening functions (8), (10), and (11), respectively.

Molière for $\phi_{TF}(r)$, namely,

$$\phi_a(r) = \sum_{i=1}^3 A_i \exp(-\alpha_i r). \quad (11)$$

The corresponding electrostatic potential (1) is given as the superposition of three Yukawa potentials and the atomic density takes the expression

$$\rho(r) = \frac{Z}{4\pi r} \sum_{i=1}^3 A_i \alpha_i^2 \exp(-\alpha_i r). \quad (12)$$

In principle, the parameters in (11) could be obtained by numerical fitting to the numerical DHFS screening function. To do this, a conventional least-squares-fitting procedure can be used to select the optimum parameters. However, proceeding in this way and using a standard minimization method, different sets of parameters were obtained from different initial estimates reflecting the existence of local minima in the function being minimized. To avoid these uncertainties in the determination of the parameters, we have adopted the procedure described below which generalizes a more crude approach previously proposed to obtain analytical Born cross sections for elastic scattering of electrons by atoms.¹⁸

The quantities

$$R_n \equiv \frac{1}{(n+1)!Z} \int r^n \rho(r) d^3r = \frac{1}{(n+1)!} \int_0^\infty r^{n+1} \phi''(r) dr \quad (13)$$

have been computed from the DHFS density for $-1 \leq n \leq 6$. Except for the factor $(n+1)!$, which is introduced for posterior purposes, R_n coincides with the radial expected values $\langle r^n \rangle$. It can be easily seen that

$$\begin{aligned} R_{-1} &= \phi'(0), \\ R_0 &= \phi(0), \\ R_n &= \frac{1}{(n-1)!} \int_0^\infty r^{n-1} \phi(r) dr \quad (n \geq 1). \end{aligned} \quad (14)$$

To determine the parameters in the screening function (11), we require the R_n values derived from it to coincide with those computed from the DHFS results for $n = -1, 0, 1, 2, 3$, and 4 . This leads to the following relations:

$$\begin{aligned} A_1 \alpha_1 + A_2 \alpha_2 + A_3 \alpha_3 &= R_{-1}, \\ A_1 + A_2 + A_3 &= 1, \\ \frac{A_1}{\alpha_1^n} + \frac{A_2}{\alpha_2^n} + \frac{A_3}{\alpha_3^n} &= R_n \quad (n = 1, 2, 3, 4). \end{aligned} \quad (15)$$

Under these conditions it is guaranteed that (i) $\phi'_a(0)$ has the correct (DHFS) value, (ii) $\phi_a(0) = 1$ (only two of the three parameters A_i need to be given), and (iii) considering screening functions as distributions, the four first moments of $\phi_a(r)$ coincide with those of the DHFS screening function. This last feature makes Born cross sections derived from (11) to practically coincide with those computed from the DHFS screening function (see Sec. III).

For neutral atoms, Eqs. (15) can be solved analytically as shown in the Appendix. However, it should be noticed that, as the α_i values have to be positive, DHFS radial ex-

TABLE I. Parameters of the analytical screening function $\phi_a(r)$. Elements indicated with an asterisk have DHFS radial expected values inconsistent with conditions (15).

Element	A_1	A_2	α_1	α_2	α_3
H 1*	-184.39	185.39	2.0027	1.9973	
He 2*	-0.2259	1.2259	5.5272	2.3992	
Li 3*	0.6045	0.3955	2.8174	0.6625	
Be 4*	0.3278	0.6722	4.5430	0.9852	
B 5*	0.2327	0.7673	5.9900	1.2135	
C 6*	0.1537	0.8463	8.0404	1.4913	
N 7*	0.0996	0.9004	10.812	1.7687	
O 8*	0.0625	0.9375	14.823	2.0403	
F 9*	0.0368	0.9632	21.400	2.3060	
Ne 10*	0.0188	0.9812	34.999	2.5662	
Na 11*	0.7444	0.2556	4.1205	0.8718	
Mg 12*	0.6423	0.3577	4.7266	1.0025	
Al 13*	0.6002	0.3998	5.1405	1.0153	
Si 14*	0.5160	0.4840	5.8492	1.1732	
P 15*	0.4387	0.5613	6.6707	1.3410	
S 16	0.5459	-0.5333	6.3703	2.5517	1.6753
Cl 17	0.7249	-0.7548	6.2118	3.3883	1.8596
Ar 18	2.1912	-2.2852	5.5470	4.5687	2.0446
K 19	0.0486	0.7759	30.260	3.1243	0.7326
Ca 20*	0.5800	0.4200	6.3218	1.0094	
Sc 21*	0.5543	0.4457	6.6328	1.1023	
Ti 22	0.0112	0.6832	99.757	4.1286	1.0090
V 23	0.0318	0.6753	42.533	3.9404	1.0533
Cr 24	0.1075	0.7162	18.959	3.0638	1.0014
Mn 25	0.0498	0.6866	31.864	3.7811	1.1279
Fe 26	0.0512	0.6995	31.825	3.7716	1.1606
Co 27	0.0500	0.7142	32.915	3.7908	1.1915
Ni 28	0.0474	0.7294	34.758	3.8299	1.2209
Cu 29	0.0771	0.7951	25.326	3.3928	1.1426
Zn 30	0.0400	0.7590	40.343	3.9465	1.2759
Ga 31	0.1083	0.7489	20.192	3.4733	1.0064
Ge 32	0.0610	0.7157	29.200	4.1252	1.1845
As 33	0.0212	0.6709	62.487	4.9502	1.3582
Se 34*	0.4836	0.5164	8.7824	1.6967	
Br 35*	0.4504	0.5496	9.3348	1.7900	
Kr 36*	0.4190	0.5810	9.9142	1.8835	
Rb 37	0.1734	0.7253	17.166	3.1103	0.7177
Sr 38	0.0336	0.7816	55.208	4.2842	0.8578
Y 39	0.0689	0.7202	31.366	4.2412	0.9472
Zr 40	0.1176	0.6581	22.054	4.0325	1.0181
Nb 41	0.2257	0.5821	14.240	2.9702	1.0170
Mo 42	0.2693	0.5763	14.044	2.8611	1.0591
Tc 43	0.2201	0.5618	15.918	3.3672	1.1548
Ru 44	0.2751	0.5943	14.314	2.7370	1.1092
Rh 45	0.2711	0.6119	14.654	2.7183	1.1234
Pd 46	0.2784	0.6067	14.645	2.6155	1.4318
Ag 47	0.2562	0.6505	15.588	2.7412	1.1408
Cd 48	0.2271	0.6155	16.914	3.0841	1.2619
In 49	0.2492	0.6440	16.155	2.8819	0.9942
Sn 50	0.2153	0.6115	17.793	3.2937	1.1478
Sb 51	0.1806	0.5767	19.875	3.8092	1.2829
Te 52	0.1308	0.5504	24.154	4.6119	1.4195
I 53	0.0588	0.5482	39.996	5.9132	1.5471
Xe 54*	0.4451	0.5549	11.805	1.7967	
Cs 55	0.2708	0.6524	16.591	2.6964	0.6814
Ba 56	0.1728	0.6845	22.397	3.4595	0.8073
La 57	0.1947	0.6384	20.764	3.4657	0.8911
Ce 58	0.1913	0.6467	21.235	3.4819	0.9011
Pr 59	0.1868	0.6558	21.803	3.5098	0.9106

Table I. (Continued).

Element	A_1	A_2	α_1	α_2	α_3
Nd 60	0.1665	0.7057	23.949	3.5199	0.8486
Pm 61	0.1624	0.7133	24.598	3.5560	0.8569
Sm 62	0.1580	0.7210	25.297	3.5963	0.8650
Eu 63	0.1538	0.7284	26.017	3.6383	0.8731
Gd 64	0.1587	0.7024	25.497	3.7364	0.9550
Tb 65	0.1453	0.7426	27.547	3.7288	0.8890
Dy 66	0.1413	0.7494	28.346	3.7763	0.8969
Ho 67	0.1374	0.7558	29.160	3.8244	0.9048
Er 68	0.1336	0.7619	29.990	3.8734	0.9128
Tm 69	0.1299	0.7680	30.835	3.9233	0.9203
Yb 70	0.1267	0.7734	31.681	3.9727	0.9288
Lu 71	0.1288	0.7528	31.353	4.0904	1.0072
Hf 72	0.1303	0.7324	31.217	4.2049	1.0946
Ta 73	0.1384	0.7096	30.077	4.2492	1.1697
W 74	0.1500	0.6871	28.630	4.2426	1.2340
Re 75	0.1608	0.6659	27.568	4.2341	1.2970
Os 76	0.1722	0.6468	26.586	4.1999	1.3535
Ir 77	0.1834	0.6306	25.734	4.1462	1.4037
Pt 78	0.2230	0.6176	22.994	3.7346	1.4428
Au 79	0.2289	0.6114	22.864	3.6914	1.4886
Hg 80	0.2098	0.6004	24.408	3.9643	1.5343
Tl 81	0.2708	0.6428	20.941	3.2456	1.1121
Pb 82	0.2380	0.6308	22.987	3.6217	1.2373
Bi 83	0.2288	0.6220	23.792	3.7796	1.2534
Po 84	0.1941	0.6105	26.695	4.2582	1.3577
At 85	0.1500	0.6031	31.840	4.9285	1.4683
Rn 86	0.0955	0.6060	43.489	5.8520	1.5736
Fr 87	0.3192	0.6233	20.015	2.9091	0.7207
Ra 88	0.2404	0.6567	24.501	3.5524	0.8376
Ac 89	0.2266	0.6422	25.684	3.7922	0.9335
Th 90	0.2176	0.6240	26.554	4.0044	1.0238
Pa 91	0.2413	0.6304	25.193	3.6780	0.9699
U 92	0.2448	0.6298	25.252	3.6397	0.9825

pected values can be inconsistent with conditions (15) which, in such a case, must be relaxed. The parameters determined following this procedure for $Z = 1-92$ are given in Table I. Elements indicated with an asterisk are those giving DHFS radial expected values inconsistent with the conditions (15); parameters for those elements have been determined by setting $A_3 = 0$ and imposing the four first conditions (15) (see Appendix).

Analytical screening functions determined in this way agree well with the DHFS results (Fig. 1). Naturally, the analytical density (12) can only partially reproduce the oscillations of the DHFS density associated with different shell contributions (Fig. 2). One may expect that an even better approximation to the DHFS screening function could be obtained from a numerical least-squares fitting using a standard minimization procedure with the parameters in Table I as initial estimates. Such a procedure has not been pursued here because the resulting parameters do not appreciably improve the quality of the fit, i.e., our parameters lie very near the least-squares minimum. Moreover, as mentioned above, conditions (15), even in the

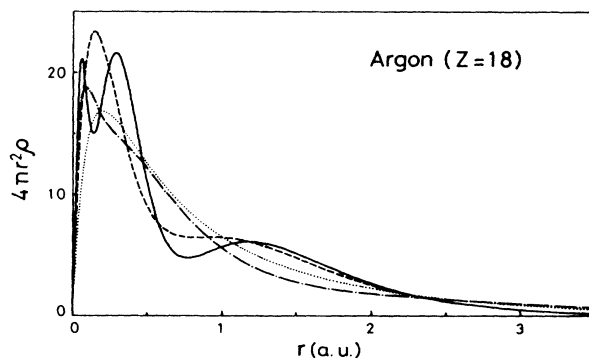


FIG. 2. Radial density for Ar ($Z = 18$). The solid curve is the DHFS density. The dash-dotted curve is the TF density derived from Molière's screening function (8). The dotted curve corresponds to the density obtained from the analytical screening function (10). The dashed curve is the analytical density (12).

noncompatible cases, ensure that the elastic Born cross sections computed from $\phi_a(r)$ practically coincide with that derived from the DHFS screening function.

III. ELASTIC BORN CROSS SECTIONS

The Born cross section for scattering of a fast particle (which, for the sake of simplification, is assumed to have unit charge and unit mass) in the atomic field (1) can be written as (see, e.g., Mott and Massey¹¹):

$$\frac{d\sigma}{d\Omega} = \frac{4Z^2}{q^4} \left[1 - \frac{F(q)}{Z} \right]^2, \quad (16)$$

where q is the momentum transfer in the collision and

$$F(q) = \int_0^\infty \frac{\sin(qr)}{qr} \rho(r) 4\pi r^2 dr \quad (17)$$

is the atomic form factor. For the density associated with our (and Molière's) analytical screening functions, the form factor takes the simple expression

$$\frac{F(q)}{Z} = \sum_{i=1}^3 A_i \alpha_i^2 / (\alpha_i^2 + q^2). \quad (18)$$

Expanding the right-hand side of Eq. (17) as a power series in q , we found

$$\frac{F(q)}{Z} = \sum_{n=0}^{\infty} (-1)^n R_{2n} q^{2n}, \quad (19)$$

with the coefficients R_n given by (13). Obviously, with the parameters of our analytical screening function satisfying (15), we guarantee that the atomic form factor (18) and its first derivatives coincide at $q=0$ with those computed from the DHFS density.

The form factors (18) are compared with the ones derived from the DHFS density and from other analytical screening functions in Fig. 3 for $Z=50$. Our analytical results differ from the DHFS numerical calculations only for relatively large momentum transfers. Although these differences might seem important, they do not appreciably

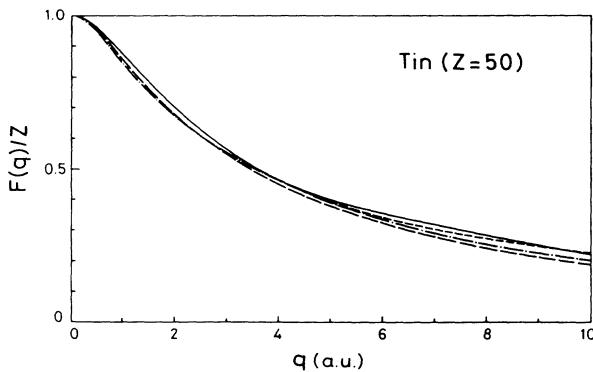


FIG. 3. Atomic form factors for Sn ($Z=50$). The solid curve is the DHFS form factor. The dash-dotted, long-dashed, and short-dashed curves correspond to form factors derived from the analytical screening functions (8), (10), and (11), respectively.

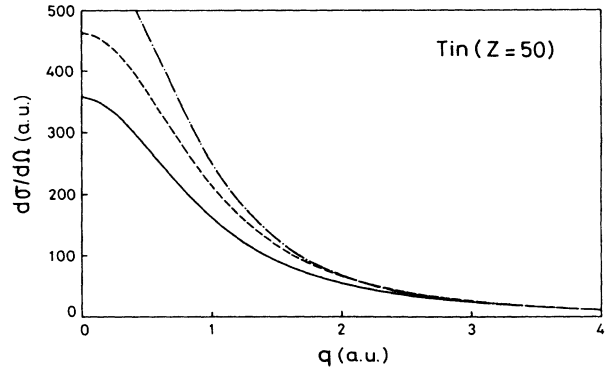


FIG. 4. Differential Born cross section for Sn ($Z=50$). The dash-dotted and dashed curves have been obtained from the analytical screening functions (8) and (10), respectively. The solid curve is the DHFS cross section. The cross section derived from the analytical density (12) coincides with the DHFS one at the drawing level.

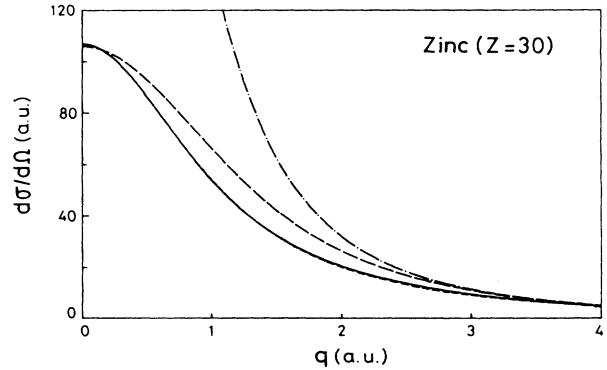


FIG. 5. Born differential cross sections for Zn ($Z=30$). The solid curve is the DHFS cross section. The correspondence between the curves and the theoretical models from which they have been obtained is the same as in Fig. 4; here the cross section derived from the analytical density (10) is shown as the short-dashed curve.

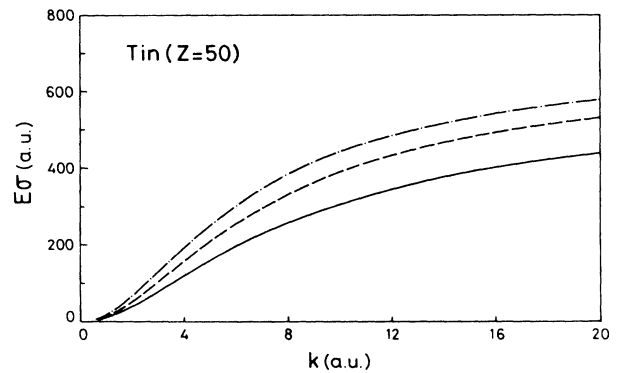


FIG. 6. Born total cross sections as functions of the momentum k of the incident particle (multiplied by $E=k^2/2$) for Sn ($Z=50$). The correspondence between the curves and the different screening functions from which they have been derived is the same as in Fig. 4.

TABLE II. Energy eigenvalues and radial expected values for tin ($Z = 50$) (atomic units). Expt.: experimental data (Ref. 19). DHFS: Relativistic self-consistent results. IPM: Relativistic eigenvalues from the analytical screening function. HFS: nonrelativistic HFS calculation. GSZ: derived from the analytical potential (9). Comparison of radial expected values from DHFS and HFS densities clearly show that relativistic effects tend to concentrate the electronic cloud near the nucleus.

	Expt.	DHFS	IPM	HFS	GSZ
$1s_{1/2}$	1073.08	1072.51	1067.64	1034.54	1042.54
$2s_{1/2}$	164.07	163.18	161.27	153.92	156.44
$2p_{1/2}$	152.73	152.91	149.97		
$2p_{3/2}$	144.38	144.29	141.57	144.42	147.70
$3s_{1/2}$	34.68	31.93	32.25	30.04	30.74
$3p_{1/2}$	29.84	27.68	27.95		
$3p_{3/2}$	26.25	26.09	26.34	26.05	26.87
$3d_{3/2}$	18.13	18.49	18.95		
$3d_{5/2}$	17.82	18.16	17.24	18.58	19.36
$4s_{1/2}$	5.02	5.24	5.16	4.88	5.16
$4p_{1/2}$		3.80	3.71		
$4p_{3/2}$	3.26	3.51	3.43	3.53	3.82
$4d_{3/2}$		1.22	1.18		
$4d_{5/2}$	0.88	1.17	1.14	1.26	1.51
$5s_{1/2}$		0.48	0.49	0.46	0.53
$5p_{1/2}$		0.23	0.22	0.22	0.57
$\langle r^{-1} \rangle$		302.20		288.59	
$\langle r^2 \rangle$		56.55		58.87	
$\langle r^4 \rangle$		629.87		701.33	

affect the resulting Born differential cross section (see Figs. 4 and 5) in which only the squared difference $[1 - F(q)/Z]^2$ weighted with q^{-4} is reflected.

The total Born cross section for an energy E of the incident particle, which can be calculated as

$$\sigma = \frac{4\pi}{E} Z^2 \int_0^{(8E)^{1/2}} \frac{1}{q^3} \left[1 - \frac{F(q)}{Z} \right]^2 dq, \quad (20)$$

becomes proportional to $1/E$ in the limit of large energies. Differences between the total cross sections derived from different screening functions are evidenced in Fig. 6 where σE is plotted as a function of the particle momentum $k = (2E)^{1/2}$. It is apparent that form factors whose derivatives at $q = 0$ differ slightly, but are otherwise rather similar, can give quite different cross sections. In particular, the TF screening function is very unsatisfactory to describe elastic collisions; this is a consequence of the unrealistically large tail of the TF electron density.

IV. IPM CALCULATIONS

In the context of the nonrelativistic IPM, atomic properties are obtained by solving the Schrödinger equation for the occupied one-electron orbitals. The relativistic IPM builds on the same grounds except for the fact that the one-electron orbitals and binding energies are found from the solution of the Dirac equation. Owing to the spherical symmetry of the potential, central field orbitals can be adopted and their radial parts obtained as the solution of the corresponding radial equations. These can be numerically solved by using standard numerical methods.

The reliability of our analytical screening functions, when adopted as the basis for IPM calculations, is

demonstrated in Table II where experimental¹⁹ and DHFS binding energies are compared with those provided by the relativistic IPM with our screening functions [using (6) as the IPM potential]. Similar agreement is found between IPM and DHFS orbitals. Nonrelativistic binding energies obtained from HFS calculations and from the IPM using the potential (9), with parameters derived by fitting the experimental ionization energies (corrected for relativistic effects⁶), are also shown in that Table.

Table II includes radial expected values $\langle r^{-1} \rangle$, $\langle r^2 \rangle$, and $\langle r^4 \rangle$, computed from the DHFS and HFS self-consistent densities. There are clear differences between the DHFS and HFS expected values arising from relativistic corrections which tend to concentrate the electronic charge near the nucleus. As a consequence, the DHFS screening function decreases faster than the HFS one with increasing radial distances. These relativistic effects on the screening functions cannot be accounted for if relativistic corrections are introduced perturbatively from nonrelativistic one-electron orbitals.

V. SUMMARY

Analytical screening functions presented here improve other alternatives previously proposed in three aspects which can be important in usual applications. Firstly, relativistic effects distorting the atomic electron cloud, and also the nuclear screened potential, are directly introduced through the DHFS model. This fact ensures reliability for large atomic numbers. Secondly, these screening functions provide cross sections for elastic scattering of charged particles in close agreement with those computed from the DHFS numerical density. In fact, the atomic

form factor derived from $\phi_a(r)$ coincides with the DHFS form factor for small momentum transfers. Lastly, the relativistic IPM with the potential (6) derived from $\phi_a(r)$ yields ionization energies and one-electron orbitals which practically coincide with the DHFS ones. This IPM potential can be useful in perturbative calculations of atomic structure and as starting potential in self-consistent calculations.

ACKNOWLEDGMENTS

This work was partially supported by the Comisión Asesora para la Investigación Científica y Técnica (Spain). Contract No. 2157/83.

APPENDIX

Equations (15) can be analytically solved in terms of the screening function parameters. After rather tedious algebraic manipulations, the constants A_i can be eliminated; the resulting equations for α_i can be written in the form

$$\begin{aligned} R_{-1} - (\alpha_1 + \alpha_2 + \alpha_3) + R_1(\alpha_1\alpha_2 + \alpha_1\alpha_3 + \alpha_2\alpha_3) \\ - R_2\alpha_1\alpha_2\alpha_3 = 0, \\ 1 - R_1(\alpha_1 + \alpha_2 + \alpha_3) + R_2(\alpha_1\alpha_2 + \alpha_1\alpha_3 + \alpha_2\alpha_3) \\ - R_3\alpha_1\alpha_2\alpha_3 = 0, \quad (A1) \\ R_1 - R_2(\alpha_1 + \alpha_2 + \alpha_3) + R_3(\alpha_1\alpha_2 + \alpha_1\alpha_3 + \alpha_2\alpha_3) \\ - R_4\alpha_1\alpha_2\alpha_3 = 0. \end{aligned}$$

These equations can now be solved for the quantities

$$\begin{aligned} a_2 &= \alpha_1 + \alpha_2 + \alpha_3, \\ a_1 &= \alpha_1\alpha_2 + \alpha_1\alpha_3 + \alpha_2\alpha_3, \\ a_0 &= \alpha_1\alpha_2\alpha_3. \end{aligned} \quad (A2)$$

Thus, the screening function parameters α_i ($i=1,2,3$) are the three solutions of the cubic equation

$$\alpha^3 + a_2\alpha^2 + a_1\alpha + a_0 = 0. \quad (A3)$$

If the three roots of (A3) are real and positive, the A_i parameters can then be computed from the first three equations of (15).

In certain cases, mainly for low atomic numbers, conditions (15) are incompatible with the DHFS radial expected values R_n , i.e., either the determinant of the coefficient matrix of (A1) is zero or some of the roots of (A3) are complex. In these cases we proceed as indicated in Sec. II, i.e., we set $A_3=0$ and impose only the first four conditions (15)—the screening function so obtained coincides with the one proposed in Ref. 18 to describe elastic scattering of electrons by atoms. Proceeding by the same steps as in the above calculation, it is easy to show that α_1 and α_2 can be obtained as the solutions of the quadratic equation

$$(R_2 - R_1^2)\alpha^2 + (R_1 - R_{-1}R_2)\alpha + (R_{-1}R_2 - 1) = 0 \quad (A4)$$

and

$$A_1 = \frac{R_{-1} - \alpha_2}{\alpha_1 - \alpha_2}, \quad A_2 = 1 - A_1. \quad (A5)$$

It should be noticed that, even when Eqs. (15) are incompatible, the form factor (18) and at least its three first derivatives coincide at $q=0$ with those computed from the DHFS self-consistent density.

¹G. Molière, Z. Naturforsch., Teil A **2**, 133 (1947).

²R. Latter, Phys. Rev. **99**, 510 (1955).

³E. K. U. Gross and R. M. Dreizler, Phys. Rev. A **20**, 1798 (1979).

⁴P. Csavinszki, Phys. Rev. **166**, 53 (1968).

⁵R. A. Bonham and T. G. Strand, J. Chem. Phys. **39**, 2200 (1963).

⁶A. E. S. Green, D. L. Sellin, and A. S. Zachor, Phys. Rev. **184**, 1 (1969).

⁷J. N. Bass, A. E. S. Green, and J. H. Wood, Adv. Quantum Chem. **7**, 263 (1973).

⁸J. C. Slater, Phys. Rev. **81**, 385 (1951).

⁹F. Herman and S. Skillman, *Atomic Structure Calculations* (Prentice-Hall, Englewood Cliffs, NJ, 1963).

¹⁰D. A. Liberman, J. T. Waber, and D. T. Cromer, Phys. Rev. **137**, A27 (1965); D. A. Liberman, D. T. Cromer, and J. T. Waber, Comput. Phys. Commun. **2**, 107 (1971).

¹¹N. F. Mott and Q. S. W. Massey, *The Theory of Atomic Collisions* (Oxford University Press, London, 1965).

¹²H. A. Bethe, Phys. Rev. **89**, 1256 (1953).

¹³W. R. Nelson, H. Hirayama, and D. W. O. Rogers, Stanford Linear Accelerator Center Internal Report No. SLAC-265 UC-32, 1985 (unpublished).

¹⁴S. M. Seltzer and M. J. Berger, Nucl. Instrum. Methods B **12**, 95 (1985).

¹⁵F. Salvat, J. D. Martínez, R. Mayol, and J. Parellada, Comput. Phys. Commun. **42**, 93 (1986).

¹⁶H. A. Bethe and R. W. Jackiw, *Intermediate Quantum Mechanics* (Benjamin, New York, 1968).

¹⁷R. Mayol, J. D. Martínez, F. Salvat, and J. Parellada, Ann. Fis. **A80**, 130 (1983).

¹⁸F. Salvat and J. Parellada, J. Phys. D **17**, 1545 (1984).

¹⁹J. A. Bearden and A. F. Burr, Rev. Mod. Phys. **19**, 125 (1967).